Available online at www.sciencedirect.com

SciVerse ScienceDirect

Procedia CIRP 00 (2014) 000–000

www.elsevier.com/locate/procedia

6th CIRP International Conference on High Performance Cutting, HPC2014

Chip Root Analysis after Machining Carbon Fiber Reinforced Plastics (CFRP) at Different Fiber Orientations

Robert Voß[a]*, Marcel Henerichs[a], Friedrich Kuster[a], Konrad Wegener[a]

[a]*Institute of Machine Tools and Manufacturing (IWF), ETH Zurich, Switzerland*

* Corresponding author. Tel.: +41 44 632 07 31; fax: +41 44 632 11 25. *E-mail address:* voss@iwf.mavt.ethz.ch

Abstract

Machining carbon fiber reinforced plastics (CFRP) is currently being heavily investigated. The main drivers come from the aviation and automotive industry. Current drilling and milling tool geometries exhibit immense wear resulting in the damage of the work piece. Detailed understanding of chip formation mechanisms when machining CFRP is paramount and enables the optimization of tool geometries in terms of tool lifetime and work piece quality. Current knowledge about CFRP chip formation mechanisms is insufficient. Chip root experiments help understanding chip formation along the cutting edge and are well understood for the machining of metals [1, 2]. Insufficient research has been performed in the field of chip formation processes when machining CFRP, especially on chip roots [3, 4, 5]. Unlike when machining metals, when machining CFRP micro-particles are generated as opposed to macro chips [4]. This fact makes it difficult to observe the CFRP chipping process, compared to metal machining. Furthermore CFRP is an anisotropic and inhomogeneous material causing machining properties to be highly dependent on the fiber orientation. This paper introduces an extensive study on CFRP chip roots for five different unidirectional fiber orientations using an orthogonal cutting test rig. Intentionally weakened work pieces have been produced. These work pieces enable truly representative cutting conditions due to a continuous cut and constant but wide range adaptable cutting speeds. Analyses of the chip roots are based on light microscopy (i), scanning electron microscopy (SEM) (ii) and micrographs (iii). In combination with previous studies in-house it qualifies to understand the wear mechanisms when machining CFRP. As a result fracture orientations, adhering abrasion particles, chip formation and chip movement allow for the understanding of CFRP chip formation.

Selection and peer-review under responsibility of the International Scientific Committee of the 6th CIRP International Conference on High Performance Cutting.

Keywords: carbon fiber reinforced plastics (CFRP); orthogonal cutting; chip root; chip formation; machining; fiber orientation

1. Introduction

Knowledge about chip formation during machining operations plays an important role when optimizing tools for lifetime and machining quality. Towards the end of the tool´s lifetime higher degrees of damage are induced onto the work piece and the machining quality decreases. Optimized tools need to meet the demands of industry for better tool lifetime and constant quality when machining carbon fiber reinforced plastics (CFRP). Consequently, it is essential to improve the insights of the mechanics of material removal of CFRP. Chip root investigation is an appropriate method to analyze chip formation and is especially well documented during metal machining [1, 2]. CFRP is a composite material which exhibits inhomogeneous and anisotropic properties dependent on fiber orientation. Additionally, CFRP does not form macro chips during conventional processing conditions but rather micro-particles in the order of dust particles (>0.5 µm). The mentioned material properties and the chip magnitude make the observation of the material removal mechanics of single carbon fibers along the cutting edge very difficult, especially during processing [6]. Many researchers use cutting parameters substantially below real application parameters used in industry in order to simplify chip formation analyses of fiber reinforced plastics (FRP) [6, 7, 8]. The simplification gives rise to the fact that at low cutting speeds, chips tend to be larger in magnitude [6]. This feature is based on the fact that carbon fiber itself is brittle and exhibits very little plastic deformation, shown among others by SHEIK-AHMAD in 2009 [9]. It is well known that higher cutting speeds cause embrittlement of the machined material,

2212-8271
Selection and peer-review under responsibility of the International Scientific Committee of the 6th CIRP International Conference on High Performance Cutting.

even in FRP [10, 11]. But it is yet to be proven that the mechanics of material removal remain the same at different cutting speeds and respectively different chip dimensions.

In the 1970s researchers theoretically described the deformation process when machining CFRP, for example by EVERSTINE and ROGERS [12]. KOPLEV et al. analyzed in 1983 the mechanical processes that occur along the cutting edge when machining CFRP. Other than SEM analysis of the work piece surface, chip cross sections, friction at the tool-work-piece contact zone and cross sections of quick stop specimens were investigated. Different types of fiber fracture during chip formation were discovered, and the machining of unidirectional CFRP is highly dependent on fiber orientation [3]. SANTHANAKRISCHNAN et al. analyzed 1988 the machining process of Glass-FRP, CFRP and Kevlar-FRP components and focused on the wear of sintered carbide tools. A strong flank wear with strap wear and considerable cutting edge rounding could be observed [13]. In the 1990s, BHATNAGAR et al. and RUMMENHÖLLER carried out extensive experiments of orthogonal cutting tests on CFRP [7, 14]. Both validate the results of KOPLEV et al. that the carbon fibers have a significant influence on the machining results than the matrix material. According to RUMMENHÖLLER, different fracture morphologies arise depending on the load condition. Two distinctive cases of fiber orientation are proposed (i) $0< \theta< 90°$ and (ii) $\theta> 90°$: For the case of $\theta=90°$, the cutting mechanisms are bending and compression. This leads to strong tool wear and poor work piece surface quality. For the case of $\theta=0°$, the cutting mechanisms are buckling and pealing with advancing crack forming in front of the cutting edge. This leads to relatively low forces and good work piece surface quality. For the case of $0< \theta< 90°$, a mixture of the aforementioned cutting mechanisms occurs [14]. SHEIKH-AHMAD defines among others, the tool geometry and material, the feed rate and the cutting speed as the most influential parameters on the machining quality of CFRP. According to SHEIKH-AHMAD, not only metal but also CFRP undergoes a change from ductile to brittle state when induced to strong deformations. By increasing the rake angle and decreasing the depth of cut, macro chips are formed due to reduced deformation of the material [9].

TAKEYAMA and ILJIMA developed a model in 1988 in which CFRP shears off along a plane at the shear angle Φ [15]. BHATNAGAR et al. extended this model by showing that the material shears off only along the fiber orientation θ. According to the research, this implies that: $\Phi=\theta$ [16]. Based on this conclusion ZHANG et al. developed a new model considering a radius at the cutting edge, wherein the bouncing-back effect of the fibers is also considered. Friction is also taken into account and the cutting tool is divided into the following three distinct regions:

- Rake face (area γ)
- Clearance face (area α)
- Cutting edge radius (area r)

This force model is valid for a fiber orientation of $0°\leq \theta\leq 90°$. An assumption is given in which the total feed and cutting forces are calculated by adding the individual forces at each area [17]. In contrast to ZHANG´s model, previous models are based on the assumption of a perfectly sharp cutting edge. The material-tool contact length for fiber orientations between $\theta=0°$ and $\theta=90°$, due to the bouncing back effect of the fibers, is assumed to be the edge radius. For fiber orientations of $\theta>90°$, this effect is assumed to be twice the cutting edge radius [17, 18].

This study presents orthogonal cutting tests including chip root analysis with application-oriented cutting parameters as follows: The cutting-speed is v_c=90 m/min, cutting width is the full material width of a_e=5 mm and the feed rate is f=0.06-0.1 mm/rotation. In contrast to the majority of publications where quick stop devices (QSD) are used, this study uses instead, intentionally weakened work pieces [6, 7, 8]. The test rig setup is based on an orthogonal turning process which enables representative cutting conditions due to a continuous cut and constant but wide range adaptable cutting speeds. The setup provides a constant fiber orientation θ during each experiment.

Nomenclature

L_z	Distance between two saw teeth	[mm]
θ	Fiber orientation	[deg]
α, β, γ	Clearance-, wedge- and rake angle	[deg]

2. Experimental Setup

The paper aims to increase tool lifetime and machining process reliability when machining CFRP by adjusting the tool macro geometry. To achieve these aims, various fundamental machining experiments are conducted on a CNC lathe. Afterwards, the work piece surface quality and resulting defects dependent on the tool geometry and the fiber orientation are analyzed.

2.1. Experimental Setup

The experimental setup for the turning tests is carried out on an Okuma LB15-II. It has been arrange to allow machining CFRP in an orthogonal turning operation at a constant fiber orientation θ. The setup enables a direct correlation between machining results and most influencing factors. Furthermore, cutting velocities between 20-500 m/min in an infinite, non-interrupted cut are possible.

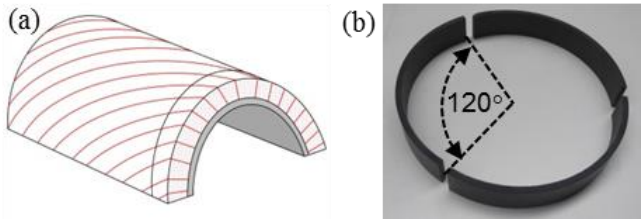

Fig. 1. (a) CFRP work piece showing exemplary fiber orientation (red lines) and single water jet cut (black line); (b) CFRP segments prior to machining.

Semi-circular shaped raw material of 1000 mm in width, 200 mm in diameter and 5 mm in wall thickness, with a single fiber orientation are manufactured for the experimental setup. Prior to machining, the raw material is cut into 120° and 55 mm wide pieces using water jet cutting. Figure 1(a) shows the semi-circular shaped raw material with an indicated fiber orientation and a single water jet cut; Figure 1(b) shows the final produced ring consisting of three segments. Producing

the work pieces this way ensures reproducible machining at a single fiber orientation per experiment.

Figure 2 shows the experimental setup where the hydraulic chuck of the CNC lathe is modified to enlarge the contact face. Machining is analyzed by a dynamometer mounted onto the tool and high speed camera recordings. An inner aluminum ring prevents the three CFRP elements from bending due to high clamping forces. Different ring diameters compensate varying CFRP ring diameters.

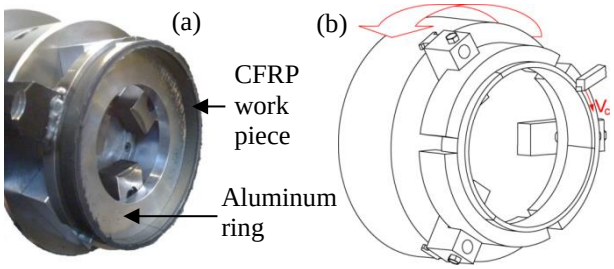

Fig. 2. (a) Test rig for orthogonal cutting tests; (b) schematic illustration.

2.2. Material

In this paper, unidirectional CFRP M21/34%/UD194/IMA-12K is used. This material is widely utilized in the aerospace industry. It contains 34 wt% high performance matrix material HexPly® M21 [*Hexcel*]. The material is well known to be difficult to machine. Both, the high fiber content (66 wt%) as well as the high toughness of the intermediate modulus fiber and matrix system cause extensive tool wear. Drilling operations of the IMA fiber result in serious delamination due to the unidirectional configuration and the difficult cutting characteristics of the fiber. A top layer of woven glass fiber, which is known to lower delamination defects, is absent in the experiments to ensure all tool wear and material defects are being generated only by the CFRP. The following table displays the mechanical properties of the machined work piece material:

Table 1. Physical properties of IMA-12K fibers.

Physical properties	Fiber	Weave/UD	Fiber Mass	Fiber volume	Laminate Density	Glass Trans. Temp.
Unit	/	/	g/m²	%	g/cm³	°C
	IMA	UD	194	59.2	1.58	195
Physical properties	Tensile	Tensile strength	Tensile modulus	Compression	Compr. strength	Compr. modulus
Unit	Method	MPa	GPa	Method	MPa	GPa
	EN 6032	3050	178	EN 2561 B	1500	146

The definition of fiber orientation θ relative to the cutting direction is illustrated in Figure 3. In the experiments, five different fiber orientations are investigated: θ=0°=180°, θ=30°, θ=60°, θ=90° and θ=150°.

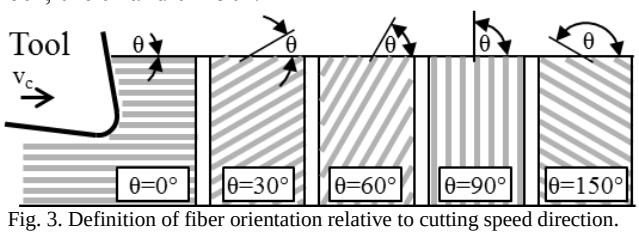

Fig. 3. Definition of fiber orientation relative to cutting speed direction.

2.3. Cutting Tools

Uncoated carbide tools of the grade H13A serve as the cutting inserts. Eight different tool geometries with varying rake and clearance angles are tested in the complete experimental series. As shown in Table 2, the rake angle γ varies from 0°-30°, the clearance angle α varies from 7°-21° and the mean cutting edge radius is r=5 µm. The initial cutting insert geometry is CCMW09T304 according to ISO standards, see (a, b) in Figure 4. Different macro geometries are created by grinding, see side view of cutting insert with adapted rake angle in Figure 4 (c).

Table 2. Cutting insert geometries.

Tool Description	**C**	**E**	**H**	**I**	**J**	**L**	**M**	**N**
Rake Angle γ	0°	10°	10°	10°	20°	20°	20°	30°
Clearance Angle α	14°	7°	14°	21°	7°	14°	21°	7°

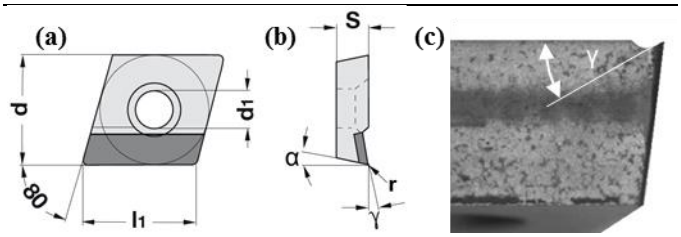

Fig. 4. Cutting Tool: (a) Top view; (b) Side view; (c) Side view: ground γ .

2.4. Experimental Procedure

The unidirectional CFRP is machined in an orthogonal turning process. The machining conditions are constant except for the rake angle γ, the clearance angle α and the varying fiber orientation θ; see Table 3.

Table 3. Machining Parameters: Orthogonal turning tests and chip root experiments.

γ ; α	**v_c**	**f**	**a_e**	**θ**	**Q`$_w$**	**V`$_w$**
deg	m/min	mm	mm	deg	mm³/mm/min	mm³/mm
0–30; 7–21	90	0.06-0.1	5	0, 30, 60, 90, 150	2700	1241

In contrast to most quick stop devices, both the cutting speed v_c=90 m/min as well as the feed f=0.06 to 0.1 mm are carried out under realistic machining conditions. The removed material per millimeter cutting edge is V`$_w$=1241 mm³/mm and the specific removal rate is Q`$_w$=2700 mm³/mm/min. The cycle time of one orthogonal turning experiment is about 25 seconds. The time necessary to undertake chip root experiment varies, dependent among others on the forces to break the chip root off the work piece.

Instead of using *ballistic methods* or *quick stop devices (QSD)*, intentionally weakened work pieces are used. Figure 5(a) shows the simplified sequence for chip root experiments in three steps. The intentionally weakened work piece is shown in step one. A parallel slit, two millimeters beneath the surface, and about twelve millimeters in length is introduced into the work piece. Before starting the experiments, the introduced slit is refilled with a steel plate to prevent the eventual root from bending due to process forces.

The CFRP is incrementally machined until the predetermined breaking area is too weak to withstand the forces. At this moment, the weakened chip breaks off and the machining process is “halted”, shown in step three.

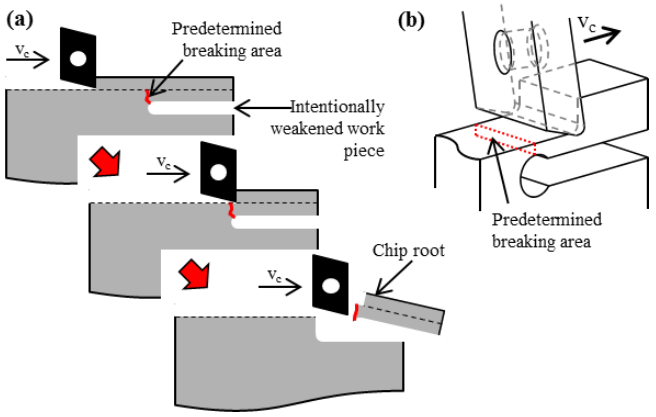

Fig. 5. Sequence of chip root generation: (a) Side view; (b) 3D.

3. Experimental Results

The results in this paper are part of a large series of experiments at the Institute of Machine Tools and Manufacturing at ETH Zurich. Focus is on work piece quality by showing process forces, CFRP surface roughness, as well as SEM picture of the chip roots and micrograph sections.

3.1. Process Forces

Force measurement has been conducted using a *Kistler* 9121 dynamometer. The force profiles for the different experiments exhibit the sample distribution, but maximum values vary. One force profile with feed-, cutting- and passive force is displayed exemplarily on the upper right side of each graph in Figure 6. The two graphs show the maximum process forces, when machining five different fiber orientations θ, plotted over the different tool geometries. The descriptions on the x-axis *C, E, H, I, J, L, M, N* denote the tool geometry and the numbers in brackets describe the rake- and the clearance angle (γ,α) respectively.

Machining unidirectional CFRP with a fiber orientation of θ=150° leads to the lowest feed forces in this experimental series, see graph in Figure 6(a). These feed forces range from 2.5 N to 30 N and are mainly dependent on the tool rake angle γ and less dependent on α. The larger the rake angle γ, the lower the feed force. The tool is being pulled between the θ=150° fibers, due to the intervention conditions and the fiber orientation relative to the cutting speed direction v_c. Machining the other four fiber orientations between θ=0° and θ=90° show completely different maximum feed forces in the range of 165 N to 870 N. It suggests that the machining and intervention conditions differ for these fiber orientations. When machining 0°≤ θ≤ 90°, the maximum feed forces seem to be highly dependent on the clearance angle α, but less dependent on the rake angle γ of the tool. For example, the combination of θ=30° and the tools *E*, *J* and *N* which exhibit the same clearance angle α=7° but an increasing rake angle of γ=10°, γ=20° and γ=30° lead to similar maximum feed forces F_f between 870 N and 830 N. On the other hand, the combination of θ=30° and the tools *E*, *H* and *I* with the same rake angle γ=10° but an increasing clearance angle of α=7°, α=14° and α=21° respectively lead to decreasing feed forces F_f from 870 N, 695 N to 610 N. In this case, an increase in clearance angle Δα=+14° leads to a reduction of feed force of about 30% at θ=30°. This amount is comparable to the feed force reduction at θ=0° of about 34%. For fiber orientations at θ=60° and θ=90°, the F_f reduction due to Δα=+14° is even higher with about 60%. The different magnitudes of maximum feed forces for the varying fiber orientations θ result from diverse effects between the CFRP fibers and the clearance face of the tool. These effects include friction, bouncing-back phenomenon dependent on fiber orientation and the amount of chips being forced under the cutting edge and along the clearance face.

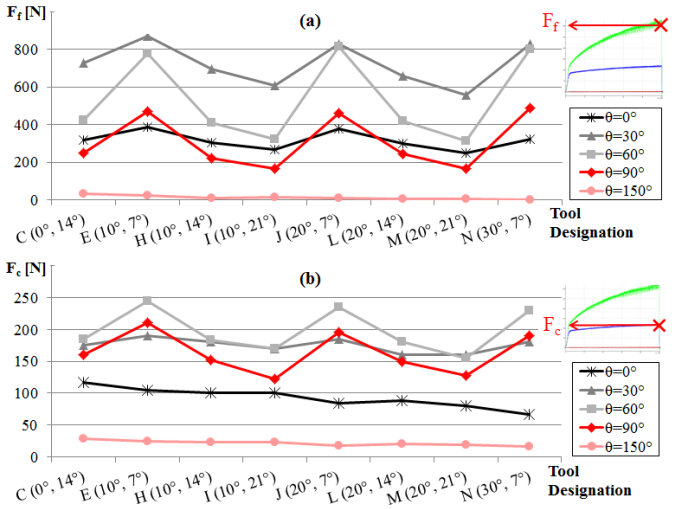

Fig. 6. Max. forces at the end of process: (a) feed forces; (b) cutting forces.

Same as for the feed forces, machining at a fiber orientation of θ=150° result in the lowest maximum cutting force F_c, see Figure 6(b). F_c at θ=60° show highest values in this experimental series especially for small clearance angles α and exceeds F_c at θ=90° of about 30 to 50 N. Unlike at θ=0° and θ=150° fiber orientations, the clearance angle has a strong influence on the cutting force for 60°≤ θ≤ 90°. By increasing the clearance angle from α=7° to α=21°, the maximum cutting force significantly decreases by 42% (θ=90°) and 34% (θ=60°) and only marginally by 14% (θ=30°), 5% (θ=0°) and ±8% (θ=150°). This indicates different mechanics of material removal or introduced material damages for fiber orientations in the range of 60°≤ θ≤ 90°. These results are in good agreement with RUMMENHÖLLER`s experimental conclusion with a case distinctive and a mixture of different cutting mechanisms [14].

3.2. Roughness

Roughness measurements are performed tangential to the direction of cut on the machined surface using a tactile Taylor-Hobson surface profiler. Measurements are performed according to DIN EN ISO 4288. Figure 7 shows mean R_a and R_z values per fiber orientation θ, each averaged from three separate measurements, and plotted according to the tool geometry.

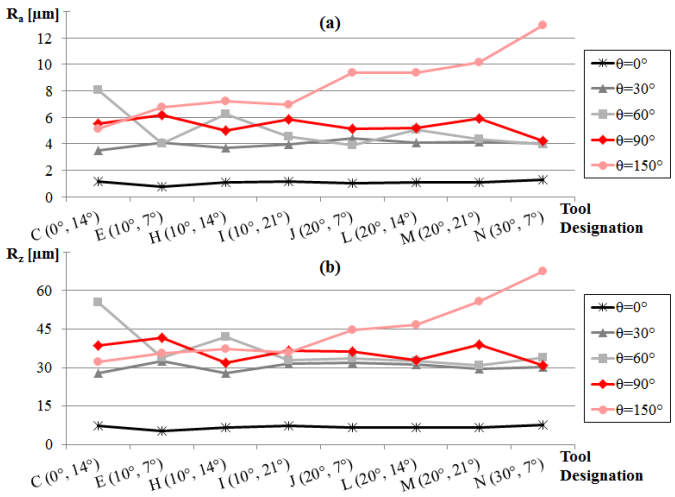

Fig. 7. Surface roughness R_a and R_z measured tangentially to v_c.

CFRP material at θ=0° shows the lowest roughness almost independent of the tool geometry, 0.8 µm≤ R_a≤ 1.3 µm. The roughness at θ=30°, θ=60° and θ=90° is somewhat higher in a range of $R_{a,\theta=30°}$=4 µm, $R_{a,\theta=60°}$=4-8 µm and $R_{a,\theta=90°}$=4-6 µm respectively. Machining at fiber orientation of θ=150° causes very poor roughness. The graph shows discrete levels of roughness depending on the rake angle. The larger the rake angle γ, the higher the surface roughness, which is almost independent of the clearance angle α. It is explainable with an initiate inter-laminar and advancing crack before breaking the bent fibers vertically, see also Figure 8: A larger rake angle bends the downstream fibers less and the inter-laminar crack penetrates further into the material before exceeding the bending strength of the fibers. At θ=60°, two phenomena are superimposed: Firstly, a small clearance angle (α=7°) leads to relatively low roughness, which is independent of the rake angle: Compare results for tools *E, J, N* in combination with θ=60° in Figure 7. Secondly, a small rake angle in combination with larger α generates a poorer surface roughness. The surface roughness at θ=30° and θ=60° behave inconsistently with regards to the clearance angle: At θ=30° the tools with a low α=7° lead to higher R_a and R_z values.

3.3. Micrographs

Micrographs longitudinal to the cutting speed direction have been prepared for each material-tool combination. Figure 8 shows a selection of the most significant results so as to increase the understanding of chip formation in accordance with the other analyzing methods. The direction of cut is shown from left to right in each picture. Machining θ=0° shows best surface quality without cracks beneath the top layer. The surface of fiber orientation θ=30° is relatively smooth and does not show cracks however, single broken and pulled out fibers are present, see Figure 8(b). Figure 8(c) and 8(d) show a comparison of θ=90° material, machined with an α=7° and α=21° tool. Micrographs at θ=60° (not displayed) and θ=90° show cracks at approximately 30 µm to 130 µm beneath the surface. For larger clearance angles α≥14° more cracks occur and some fibers are broken multiple times; compare Figure 8(c) and Figure 8(d). This may be explained by lower feed forces for α≥ 14° which compress and reinforce the fiber bundles. The observed cracks in turn provide an explanation for decreasing cutting forces due to material weakening. The different cracks result from several work piece rotations since the feed rate f=30 µm is smaller than the cracks length of up to 130µm.

Machining at θ=150° leads to saw-tooth profiles on the surface, see Figure 8(e) and (f). The micrographs validate the roughness results in which the size of a single saw-tooth is mainly dependent on the rake angle γ. The difference between (e) and (f) is an increased rake angle Δγ=+20°, which leads in average to a 30% longer distance between two teeth in cutting direction (L_z).

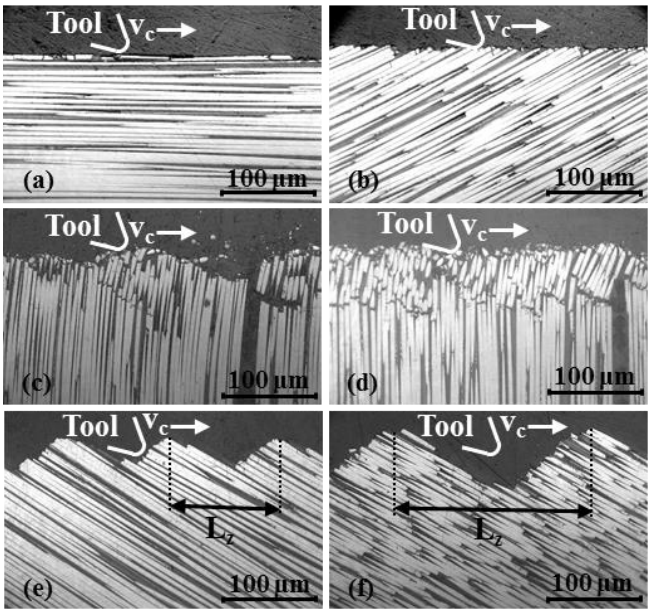

Fig. 8. Micrographs of CFRP surface: (a) θ=0° H(10°,14°); (b) θ=30° H(10°,14°); (c) θ=90° J(20°,7°); (d) θ=90° M(20°,21°); (e) θ=150° C(0°,14°); (f) θ=150° L(20°,14°).

3.4. Chip Roots

Figure 9 shows SEM pictures of chip roots at each respective fiber orientation. The line of sight of the SEM pictures is explained in the upper left sketch: As indicated, the cutting direction in pictures b, c, d, e and f shows from front to back while the focus in the middle of the pictures is on the "frozen" machining process ("*step*"). Interrupting the machining process at fiber orientations 0° ≤ θ ≤ 90° results in various kinds of *steps*. However at θ=150° (f) the cutting insert generates no step but gapping fibers due to opposite intervention conditions. The tool cleaves the θ=150° fibers inter-laminar and creates a gaping crack.

On the left hand side in Figure 9(b) a slight dark shadow in cutting direction represents a matrix layer perpendicular to the surface. In this matrix layer, the *step* looks sticky with abrasion particles. The fiber stumps are visible in the upper region of the θ=0° steps (b). In the same area at θ=30° (c), θ=60° (d) and θ=90° (d) the original fiber orientations are observable, since the fibers are uncovered. Coincidentally, a 100 µm wide pre-machined block of fibers still sticks to the *step* in picture (d) and is not completely removed. The removal mechanism for θ=30° and θ=60° fiber orientations shows crushing of fibers at the chip root bottom and removal of blocks after an inter-laminar shearing. Furthermore not just uncovered but even exposed fibers are visible at θ=150° (f).

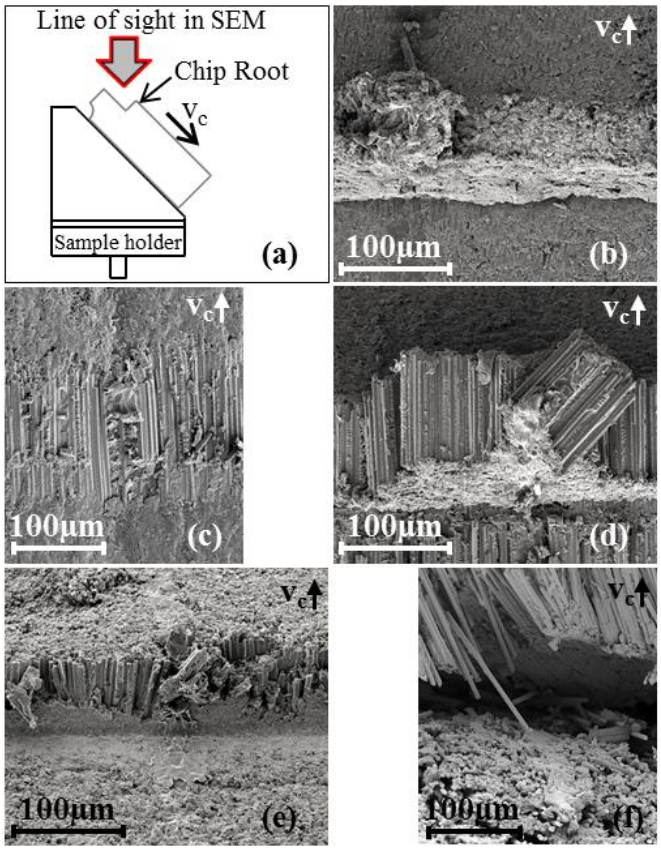

Fig. 9. Chip Roots: (a) sketch for clarification; SEM pictures: θ=0° (b), θ=30° (c), θ=60° (d), θ=90° (e), θ=150° (f).

In the lower area of each step (b), (d) and (e), chips and abrasion particles seem to be compressed and fill the transition between step and final machined surface; this is in the order of the cutting edge radius. The height of these compressed particles is about 10-40 µm dependent on the fiber orientation θ. At fiber orientation of θ=30° in picture (c), the angle of the step seems to be too flat to compress particles at the transition between the generated surface and the uncovered fibers. Both, the previous surface in the back as well as the final generated surface in front are smeared with abrasive and matrix particles at 0°≤θ≤90°. These observations indicate particles being forced under and along the clearance face of the tool. In contrast to θ=60° and θ=90°, SEM pictures of θ=0° (a) show a clear separation between compressed particles and the final generated surface. It indicates the covering layer is much thinner at θ=0°, which consequently leads to a low surface roughness (Ra~1 µm).

4. Conclusion

Intentionally weakened work pieces are sufficient to generate chip roots with realistic process parameters when machining CFRP. At θ=0°, θ=60°, θ=90° where the cutting inserts face a certain step, show compressed abrasion particles in the lower transition area of the steps. Analysis shows that the height of the compressed particles is about the radius of the worn cutting edge. As a result the particles are unable to convey over the tool´s rake face and are instead forced under the tool´s clearance face and smear along the machined surface. At θ=30° and θ=60°, the chip removal mechanism is mainly inter-laminar sliding along the fiber orientation θ coherently in form of a block.

At θ=150°, pealing occurs due to an advancing inter-laminar crack and bending of the fibers along the cutting direction until the maximum bending stress is surpassed. This results in low process forces and high surface roughness. The size of the arising saw teeth is mainly dependent on the rake angle γ.

In general, high roughness indicates material cracks, saw teeth on the surface or partially broken fibers. Low roughness does not guarantee that there are no defects in the surface. Although the surface is smeared with abrasive particles and thus relatively smooth, underlying cracks may exist. The machined surface at 0°≤θ≤90° is highly smeared with abrasive particles. Material defects like cracks, as well as broken and pulled out fibers need to be considered under this smeared layer. Especially at θ=60° and θ=90°, cracks occur due to loading the fibers owing to bending. Small clearance angles α reduce the probability of cracking because of higher feed forces F_f which reinforce the fibers.

References

[1] Ellis J, Kirk R, Barrow G; 1969; The development of a quick-stop device for metal cutting research; International J. of Machine Tool Design and Research; Elsevier, 9, 321-339.
[2] Philip PK; 1971; Study of the Performance Characteristics of an Explosive Quick-Stop Device for Freezing Cutting Action; International J. of Machine Tool Design and Research; Elsevier, 11, 133-144.
[3] Koplev A., Lystrup A, Vorm T.; 1983; The cutting process, chips, and cutting forces in machining CFRP; Composites; Elsevier, 14, 371-376.
[4] Bhatnagar et al.; 1995; On the machining of fiber reinforced plastic (FRP) composite laminates; International J. of Machine Tools and Manufacture; Elsevier, 35, 701-716.
[5] Arola D, Ramulu M, Wang D; 1996; Chip formation in orthogonal trimming of graphite/epoxy composite; Composites Part A: applied science and manufacturing; Elsevier, 27, 121-133.
[6] Azmi AI; 2013; Chip formation studies in machining fibre reinforced polymer composites; Int. J. Materials and Product Technology, Vol 46, No. 1, 32-46.
[7] Bhatnagar et al.; 1995; On the machining of FRP composite laminates; Int. J. of Machine Tools and Manufacturing; Elsevier, 35, 701-716.
[8] Arola D, Ramulu M., Wang D; 1996; Chip formation in orthogonal trimming of graphite/epoxy composite; Composites Part A: applied science and manufacturing; Elsevier, 27, 121-133.
[9] Sheikh-Ahmad, J. Y.; 2009; Book: Machining of Polymer Composites; Publisher: Springer; Abu Dhabi.
[10] Karman Th; 1911; Festigkeitsversuche unter allseitigem Druck;. Z. VDI Jg. 55 H. 42, 1749–1757.
[11] Böker R; 1915; Die Mechanik der bleibenden Formänderung in kristallinisch aufgebauten Körpern; Verhandl. Deut. Ingr. Mitt. Forsch.; 175, 1–51.
[12] Everstine GC; Rogers TG; 1970; A Theory of Machining of Fiber-Reinforced Materials, Journal of Composite Materials; 5; 94-106.
[13] Santhanakrishnan G, Krishnamurthy R, Malhotra SK; 1988; Machinability Characteristics of Fibre Reinforced Plastics Composites; Journal of Mechanical Working Technology; 17; 195-204.
[14] Rummenhöller S; 1996; Werkstofforientierte Prozeßauslegung für das Fräsen von kohlenstofffaserverstärkten Kunststoffen; PhD Thesis; RWTH Aachen.
[15] Takeyama H, Iijima N; 1988; Machinability of glass-fiber reinforced plastics and application of ultrasonic machining; CIRP Annals; 37; 93-96.
[16] Bhatnagar N, Ramakrishnan N, Naik NK, Komanduri R; 1995; On the machining of fiber reinforced plastic (FRP) composite laminates“; Int. J of Machine Tools and Manufacture; 35; 701–716.
[17] Zhang LC; Zhang HJ; Wang XM; 2001; A Force Prediction Model for Cutting Unidirectional Fiber-Reinforced Plastics; Machining Science and Technology: An International Journal; 5, 293-305.
[18] Davim JP; 2010; Machining Composite Materials; Wiley;ISTE; London.